Two Functionally Distinct Forms of Guanosine Cyclic 3',5'-Phosphate Stimulated Cation Channels in a Bovine Rod Photoreceptor Disk Preparation†

L. Bruce Pearce,‡ Roger D. Calhoon, Paul R. Burns, Alice Vincent, and Stanley M. Goldin*
Department of Biological Chemistry and Molecular Pharmacology, Harvard Medical School, Boston, Massachusetts 02115
Received September 4, 1987; Revised Manuscript Received February 18, 1988

ABSTRACT: Cyclic nucleotide stimulated efflux of $^{22}Na^+$ and $^{45}Ca^{2+}$ from a purified bovine rod outer segment disk preparation was measured on the 25–100-ms time scale by a novel rapid superfusion method. Activation of cation efflux by 8-bromoguanosine cyclic 3',5'-phosphate (8-Br-cGMP) was maximal within 25 ms. Over a wide range of concentrations of 8-Br-cGMP, the kinetics of termination of efflux precisely conformed to the sum of two exponential decay processes: a rapid phase (decay constant of 200 ms) and a slower phase (decay constant of 1.6 s). The kinetics of the biphasic decay of efflux cannot be explained by depletion of a pool of releaseable ^{22}Na but appear to reflect an intrinsic process for inactivation of the channels. 8-Br-cGMP-stimulated release of actively accumulated ^{45}Ca exhibited identical biphasic decay kinetics. The maximum rate of Ca release [5 nmol·(mg of disk protein)$^{-1}$·min^{-1}] may be sufficient to produce a 1 μM change in local cytoplasmic [Ca] within 20 ms. The Ca:Na selectivity ratio is ~0.5:1 for both decay phases. 8-Br-cGMP demonstrated a lower potency (EC_{50} of 8.4 μM vs 2.8 μM) but a higher degree of cooperativity in its activation of the rapid vs the slower decay phase of ^{22}Na efflux. The slower phase of decay was selectively inhibited by 25 μM *l-cis*-diltiazem, a relatively weak inhibitor of the rapid decay phase. Sodium ion (5–10 mM) selectively inhibited the rapid decay phase of 8-Br-cGMP-stimulated ^{45}Ca release. These two kinetically and pharmacologically distinct phases of decay are hypothesized to represent two functionally distinct forms of cGMP-stimulated cation channels.

Photolysis of rhodopsin in the disk membrane of vertebrate rod photoreceptor outer segments (ROS)[1] initiates a sequence of events leading to the hyperpolarization of the ROS plasma membrane [reviewed by Stryer (1986)]. The recent discovery and characterization of cGMP-activated ion channels in the ROS plasma membrane (Fesenko, 1985; Yau & Nakatani, 1985) strongly favor the hypothesis that the reduction of free cytoplasmic cGMP levels produces this rapid hyperpolarization via a light-induced activation of a cyclic nucleotide phosphodiesterase.

Photoreceptor disks are also hypothesized to contain cGMP-sensitive channels. This is based on observations of cGMP-stimulated Ca^{2+} uptake in frozen and sonicated ROS membrane vesicles (Caretta & Cavagionni, 1983), cGMP-induced release of Ca^{2+} from osmotically lysed or permeabilized ROS (Koch & Kaupp, 1985), and cGMP-stimulated release of Ca^{2+} from a purified photoreceptor disk preparation (Puckett & Goldin, 1986). In the latter study, Ca^{2+} was released from a Ca^{2+} pool actively accumulated by a separate ATP-dependent Ca^{2+} uptake activity (Puckett et al., 1985).

Cytoplasmic free [Ca^{2+}] in ROS is submicromolar (McNaughton et al., 1986; Miller & Korenbrot, 1986), and disks contain high levels of Ca^{2+}, in excess of 2 mM (Kaupp & Schnetkamp, 1982; Schroder & Fain, 1984). On the basis of this and the above, it would be expected that the light-induced reduction in cytoplasmic [cGMP] would attenuate Ca^{2+} efflux from the disk lumen into the cytoplasm, in parallel with the direct effect of cGMP on the cation conductance of the ROS plasma membrane. The putatative disk-associated cGMP-activated channels may contribute to the short- and/or long-term regulation of phototransduction, but the physiological role of this cGMP-activated Ca^{2+} release process is as yet undefined.

Significant similarities exist in terms of the pharmacology of activation and inhibition of the cGMP-activated conductances of patch-clamped plasma membranes (Fesenko et al., 1985; Stern et al., 1986) and activation and inhibition of cGMP-sensitive Ca^{2+} efflux hypothesized to occur from disks (Koch & Kaupp, 1985; Puckett & Goldin, 1986). However, it is not known whether the putative cGMP-sensitive channels gating Ca^{2+} efflux are identical molecular species with those of the plasma membrane. Furthermore, observations from our laboratory (Puckett & Goldin, 1986) indicated that cGMP-stimulated Ca^{2+} release from purified bovine disks terminates by a mechanism suggestive of inactivation of the release activity, which contrasts with the observation that the cGMP-stimulated conductance of plasma membranes remains activated for prolonged periods in the presence of cGMP (Fesenko, 1985; Haynes et al., 1986; Zimmerman & Baylor, 1986). This may reflect the existence of multiple functional states of a single class of channels or, alternatively, multiple molecularly distinct classes of cGMP-activated channels in ROS.

A barrier to direct comparison of the properties of the ion channels putatively associated with disks with those of the ROS

† This work was supported by a grant from the National Institutes of Health (GM 35423) and by a Rita Allen scholars award to S.M.G. L.B.P. was supported in part by a National Research Service award fellowship (NS 07467) from the National Institutes of Health and by a U.S. Public Health Service training grant (NS 07009) from the National Institutes of Health.

* Address correspondence to this author at the Department of Biological Chemistry and Molecular Pharmacology, Harvard Medical School, 250 Longwood Ave., Boston, MA 02115.

‡ Present address: Department of Pharmacology and Experimental Therapeutics, Boston University School of Medicine, 80 E. Concord St., Boston, MA 02118.

[1] Abbreviations: ATP, adenosine 5'-triphosphate; cGMP, guanosine cyclic 3',5'-phosphate; 8-Br-cGMP, 8-bromoguanosine cyclic 3',5'-phosphate; ROS, rod outer segment(s); MOPS, 3-(*N*-morpholino)-propanesulfonic acid; SC filter, 8-μm pore size membrane filter manufactured by Millipore Corp.; GF/F filter, glass fiber depth filter with submicron particle retention capability, Whatman Corp.; TCA, trichloroacetic acid.

0006-2960/88/0427-4396$01.50/0

plasma membrane is that direct electrophysiological measurements (e.g., patch-clamp recordings) have not yet been performed on disks, and the time resolution to date for characterization of the putative disk-associated conductance (Koch & Kaupp, 1985; Puckett & Goldin, 1986; Schnetkamp, 1987) is slow relative to electrophysiological methods. We report here the use of a novel rapid superfusion system to study the cGMP-stimulated movement of $^{22}Na^+$ and $^{45}Ca^{2+}$ across the membranes of a purified bovine disk preparation. The time resolution of this method (25–100 ms) enables characterization of the kinetics and magnitude of ion fluxes on the time scale of the early events of phototransduction. We observe that the putative disk-associated channels conduct Na^+ and other monovalent cations in addition to Ca^{2+}, as is the case for the relatively nonselective cGMP-sensitive cation channels of the ROS plasma membrane (Yau & Nakatani, 1984; Hodgkin et al., 1985). The measurement of the gating of Na^+ in addition to Ca^{2+} avoids potential complications encountered in the latter case due to Ca^{2+} binding to the disks and the presence of competing transport activities such as Na^+/Ca^{2+} exchange. We detect two distinct and transient components of the cGMP-stimulated response that differ in kinetics of decay, 8-Br-cGMP concentration dependence for activation, and sensitivity to inhibition by Na^+ and *l-cis*-diltiazem. A preliminary account of portions of this work has appeared (Pearce et al., 1987).

Experimental Procedures

Amiloride, MgATP, cAMP, cGMP, and 8-Br-cGMP were from Sigma Chemical Co. (St. Louis, MO). All other chemicals were of the highest purity available.

Isolation of Purified Bovine Rod Outer Segment Disks. Disks were prepared in dim red light from frozen retinas (Hormel) using the procedure described by Puckett and Goldin (1985). Briefly, osmotically intact crude disks were obtained from bovine retinal rod outer segments by hypoosmotic shock, floated on a 5% Ficoll 400 solution, and separated into two distinct components, the "R-band" and the "W-band", on a linear Ficoll density gradient. The major component was the R-band and comprises the isolated disks. Disks (8–15 mg of protein/mL) were stored in the dark at 4 °C in buffer A (0.1 M KH_2PO_4, 60 mM NaOH, and 5 mM 2-mercaptoethanol, pH 7.0) for up to 4 weeks without loss of activity.

Disk preparations purified from fresh rather than frozen retinas, as previously described (Puckett & Goldin, 1985), exhibit similar Ca^{2+} transport properties. Frozen retinas were employed in the current study, however, for convenience.

Rapid Superfusion System. By the means described below and illustrated here, chemical excitation of vesicle-associated, cGMP-activated channels was experimentally controlled in analogy with the way an electrophysiologist controls electrical excitation of voltage-gated ion channels. The rapid superfusion system evolved from a design described by Forbush (1984). The major modifications entailed the design of new circuitry for programming the rapid introduction and removal of agonist and/or antagonist (Figure 1) and the development of a new superfusion chamber/membrane filter system to house the valves and membrane vesicles (Figure 2).

Buffer solutions (with and without cyclic nucleotide) were held in a pair of 200-mL stainless-steel chambers (Alloy Products Corp.) containing superfusate buffer. The two solutions ("buffer" and "drug") were separately delivered under nitrogen pressure (60–110 psi) via Teflon tubing (3 mm o.d. × 1.5 mm i.d.) to the inlets of each of two Series 9 high-speed solenoid valves (~2-ms response time; General Valve Corp., Fairfield, NJ). A few micrograms of purified disk membrane

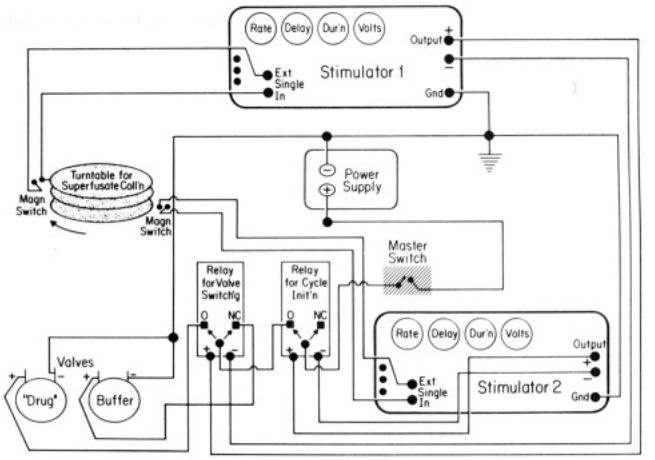

FIGURE 1: Schematic diagram of the superfusion system and the circuitry for programming the delivery of nucleotide ("drug") to the disk vesicle preparation retained on filters inside the valve housing. See the text for further details.

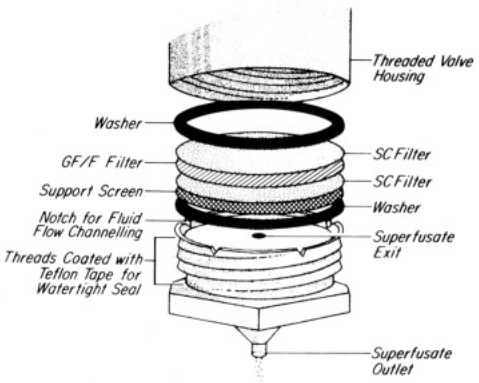

FIGURE 2: Exploded diagram of the housing containing the purified disk membrane vesicles retained on the glass fiber (GF/F) filter. See the text for further details.

vesicles, preloaded with $^{22}Na^+$ or $^{45}Ca^{2+}$, was retained within the housing in the center of a 6-mm-diameter glass fiber filter sandwiched between a pair of 6-mm-diameter nitrocellulose filters (Figure 2). The valves are housed in a custom-designed stainless-steel superfusion chamber [the entire valve/housing assembly is now commercially available (part 9-352-900) from General Valve Corp.]. The valves are configured in the housing like the two valves of an automobile internal combustion engine cylinder (not illustrated); they deliver pressurized solution above the filters, which uniformly superfuses through the membrane vesicles and is channeled through a narrow outlet (Figure 2). The superfusate exits in an continuous stream at a high flow rate (several milliliters per second), and the "dead volume" of the superfusion chamber is only ~20 μL—this ensured rapid introduction to and removal of cyclic nucleotide from the vesicles (~15-ms solution change time).

Superfusate, containing radiolabeled cations leaving the intravesicular space via cGMP-sensitive channels, was continuously collected in closely juxtaposed glass vials ($^1/_2$ dram shell vials; Rochester Scientific, Rochester, NY) mounted on the perimeter of a phonograph turntable (the entire circumference of an 11-in.-diameter platter holds ~63 vials). Collection intervals of 56 ms/fraction correspond to a turntable speed of 16 rpm; 33 rpm generates 26-ms fractions, and 78 rpm = 11.3 ms). Collection intervals greater than 56 ms but less than 0.5 s employed an external variable-speed motor geared to the turntable.

The solenoid valves either were controlled manually (0.5-s fractions) or were controlled by the circuitry shown in Figure 1. The switch between the two solutions (i.e., the introduction or removal of cyclic nucleotide) was generated by the simultaneous opening of one solenoid valve and closing of the other. In both the manual and automatic modes, the valves were operated through two high-speed mercury-wetted contact relays (GI Clare HGJM; Newark Electronics, Chicago, IL) by two simulators (Model S44; Grass Medical Instruments, Inc.). The stimulators each delivered a 5-V square-wave voltage output that activates each of two relays that connect the valves to a 12-V direct-current power supply: the first relay controls the valve switching, and the other controls the initiation of the stimulus and the superfusate collection cycle by providing the source voltage to the first relay connected in series.

The collection of superfusate was synchronized with solution delivery to the vesicles by initiating the "stimulus protocol" via magnetic reed switches that sense the position of permanent magnets fixed to the rotating turntable. The magnetic reed switches are connected to the "sync in" circuit of each stimulator. This configuration allows flexibility with regard to the stimulation protocol.

Loading Purified Disks with $^{22}Na^+$ for Efflux Measurements. The method was designed to provide for maximum specific activity of $^{22}Na^+$ in a minimal volume of R-band disks. Sections (2.5 cm) of 200-μL glass micropipets (4624; Clay Adams, Parsippany, NJ) were heat-sealed at one end, and 200 μCi (20 μL) of $^{22}Na^+$ (1000 Ci/g; New England Nuclear, Cambridge, MA) was added with a 50-μL Hamilton syringe to the bottom of this tube and dried overnight at 90 °C. The tube was placed on ice; purified disks (80 μg of protein in 5–10 μL of buffer A) were added to the bottom of the tube using a 5-μL Hamilton syringe. The tube was shaken gently on a rotating table for 4–24 h at 4 °C to allow equilibration of $^{22}Na^+$. The disks were handled in dim red light (Kodak 1 safelight filter, 15 W).

$^{22}Na^+$ Efflux Measurements. All procedures were performed in the light at ambient temperature (24 °C) except where noted. Nitrocellulose filters (SC, 25-mm diameter; Millipore Corp., Bedford, MA) were prerinsed as follows to remove incorporated detergent. Bio-Beads (Bio-Rad Corp.) were washed with methanol as previously described (Kashara & Hinkle, 1977). Eight SC filters were placed in a slurry of 1.8 g of Bio-Beads in 6 mL of distilled water in a sealed 60 × 15 mm plastic petri dish and subjected to gentle agitation on a laboratory rotator overnight at room temperature. Small (6-mm diameter) circles were then cut from the filters with a stainless-steel punch; the circles were then dried and could be stored indefinitely. Whatman 25-mm GF/F filters were not prerinsed before 6-mm circles were cut.

The filter sandwich (Millipore SC, Whatman GF/F, Millipore SC) was prerinsed with 1 mL of ice-cold buffer A and held between two stainless-steel washers within a loading chamber in the same configuration shown in Figure 2. An aliquot of disks loaded with $^{22}Na^+$ (8 μg of protein in 0.5–1.0 μL) is retained within the center 3-mm region of the filter sandwich (a tight seal between the washers and the edge of the filter sandwich restricted the region retaining the disks to the center of the filters). Disks were loaded onto the Millipore side of an already assembled filter sandwich, but the disks penetrate the first Millipore filter and are retained on the glass fiber filter (the "meat" of the sandwich). Disk vesicles trapped on the filters were washed with 1 mL of ice-cold buffer A delivered from a syringe, to remove most of the extravesicular $^{22}Na^+$. The filter sandwich containing trapped disks was then transferred to the superfusion chamber/valve assembly and placed on a stainless-steel washer within the chamber, with the disks facing the mixing chamber between the two valves (Figure 2). A stainless-steel mesh screen (400 mesh) is placed within the chamber followed by an additional stainless-steel washer, and the threaded efflux outlet fitting is used to secure the filters in place (Figure 2). Once secured within the chamber, the disks are superfused for 5 s with buffer (25 mL) to more completely remove excess radiolabel and for determination of superfusate flow rate (4–6 mL/s was the acceptable range). The cyclic nucleotide superfusion protocol was then immediately initiated.

Manual collections of superfusate (0.5-s fractions) were timed with an electronic metronome. These fractions were collected directly in shell vials (15 × 45 mm). Fractions collected at 10–50-ms intervals were collected directly into the shell vials on the rotating turntable and transferred to another set of vials for γ radiation counting. Following constant superfusion with cyclic nucleotide, the filter sandwich with trapped disk vesicles was removed immediately and counted to determine the $^{22}Na^+$ remaining associated with the disks. The amount of $^{22}Na^+$ released into the superfusate and collected in each fraction was expressed as a percentage of the total $^{22}Na^+$ initially associated with the disks.

$^{45}Ca^{2+}$ Efflux Measurement. The protocols for $^{45}Ca^{2+}$ efflux measurement were similar to that for the $^{22}Na^+$ efflux studies, with the following differences. A lower specific activity of commercially available $^{45}Ca^{2+}$ (New England Nuclear NEZ-013, ~25–35 Ci/g) limited the superfusate fraction collection interval to ~90 ms, to obtain enough dpm per fraction to permit reliable measurements. Because phosphate ion binds to and precipitates Ca^{2+}, the disk vesicles were washed and resuspended in phosphate-free buffer B (0.15 M KCl, 15 mM MOPS, and 5 mM 2-mercaptoethanol, titrated to pH 7.0 with KOH) by the following procedure, performed under dim red light at 0–4 °C. Purified disk vesicles, 4–6 mg (stored in buffer A as described above), were diluted into 35 mL of buffer B. The suspension was subjected to centrifugation in a Sorvall SS 34 rotor (Du Pont/Sorvall, Newtown, CT) at 17 500 rpm for 30 min. The pellet was resuspended in 35 mL of buffer B, and the centrifugation was repeated. The final pellet was resuspended to a [protein] of ~10 mg/mL in buffer B and incubated overnight in the dark at 4 °C.

Disks were actively loaded with $^{45}Ca^{2+}$ under ambient light by the following modifications of the procedure of Puckett et al. (1985). Disks in buffer B, prepared and stored as above, were added to a buffer B solution in a 5 × 50 mm culture tube such that the final concentration of MgATP was 2 mM; 25–35 Ci/g of $^{45}Ca^{2+}$, 0.3 mM; [$MgCl_2$], 5.5 mM; [disk protein], 1.25 mg/mL; and a final volume of 40 μL. This suspension was incubated for 30 min at 37 °C; 8 μL of the suspension was withdrawn and diluted into 40 μL of buffer B. The diluted suspension was then loaded onto the filter stack as in the $^{22}Na^+$ protocol described above; the filter stack in the loading chamber was rinsed with 3–300-μL aliquots of buffer B to remove most of the extravesicular $^{45}Ca^{2+}$.

Subsequent steps were the same as detailed above in the $^{22}Na^+$ efflux measurement protocol, but buffer B was substituted for buffer A, the nitrogen pressure was 60 psi, and the flow rate was 2–3 mL/s. Fractions were transferred to scintillation vials, ~10 volumes of Hydrofluor (National Diagnostics, Manville, NJ) were added, and the samples were counted in a β scintillation counter. Total levels of $^{45}Ca^{2+}$ incorporated into the disk vesicles were determined by sub-

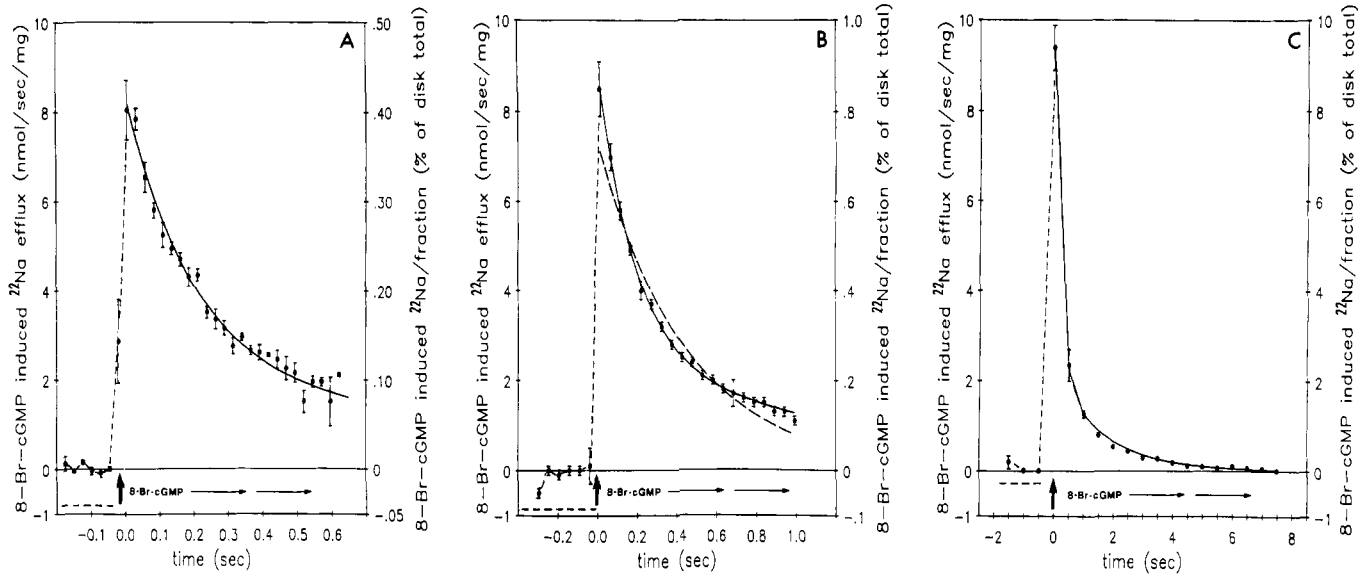

FIGURE 3: Transient 8-Br-cGMP-stimulated $^{22}Na^+$ efflux from the purified disk preparation. Disks (8 μg of protein) were preloaded with $^{22}Na^+$ and retained on microporous filters in the superfusion chamber. The disks were initially superfused with buffer; the vertical arrows denote the point of immediate switch to continuous superfusion with 25 μM 8-Br-cGMP. The effluent containing released $^{22}Na^+$ (termed the "superfusate") was collected as discrete fractions (●). Panel A displays fractions continuously collected at 26-ms intervals; panel B, 53-ms intervals; panel C, 500-ms intervals. The solid curves denote the best fit of the decay of 8-Br-cGMP-stimulated $^{22}Na^+$ release to biphasic exponential kinetics (eq 1 in text), resulting in decay constants of $p = 0.2$ s and $q = 1.6$ s. The dashed curve (----) of panel B is the best fit of the data to a single-exponential decay, with a resulting time constant of 0.45 s. The scalar value of $^{22}Na^+$ efflux denoted by the dashed horizontal lines (lower left portions of panels A–C) represents the "basal" level of $^{22}Na^+$ efflux prior to stimulation with 8-Br-cGMP. Each time point was an average of multiple experiments (vertical bars denote SEM): panel A, $n = 4$; panel B, $n = 3$; panel C, $n = 2$.

jecting the filter stack to β counting after the superfusion was completed.

To determine the effect of Na^+ on cyclic nucleotide stimulated $^{45}Ca^{2+}$ efflux, varying concentrations of NaCl were substituted for equimolar amounts of KCl in buffer B. This modified buffer was then substituted for buffer B in washing the disks free of phosphate, actively loading the disks with $^{45}Ca^{2+}$, and performing the superfusion.

Experiments were performed in parallel in which the disks were passively equilibrated overnight at 0 °C with selected concentrations of $^{45}Ca^{2+}$ in the absence of MgATP and in Na-free buffer B. The specific activity of $^{45}Ca^{2+}$ employed was the same as for the active loading experiments.

Actions of Amiloride and l-cis-Diltiazem. To determine the effect of amiloride and *l-cis*-diltiazem on cyclic nucleotide stimulated $^{22}Na^+$ or $^{45}Ca^{2+}$ efflux, each drug was added at the indicated concentration to the radioisotopically loaded disk suspension and preincubated for at least 30 min at 0 °C. Each drug was maintained at the indicated concentration in all subsequent wash solutions and in both superfusion buffer reservoirs.

Protein Determinations. Protein content of samples was determined by using a modification of the Lowry protein assay that precipitates the protein with TCA in the presence of deoxycholate (Bensadoun & Weinstein, 1976).

Data Analysis. The RS/1 mathematical modeling and curve-fitting software package for the IBM PC-AT or full compatibles (BBN Software Products Corp., Cambridge, MA) was employed for analysis of the decay kinetics; statistical analysis by RS/1 of the precision of curve fitting employed the "F-ratio" test (Draper & Smith, 1966). More basic data entry, averaging, and statistics was performed by the computer spreadsheet Lotus 1-2-3 (Lotus Development Corp., Cambridge, MA).

Results

Rapid, Transient Release of Monovalent Cations from the Disk Preparation. As resolved on the subsecond time scale by rapid superfusion, both cGMP and 8-Br-cGMP activate a Na^+ transport activity in the purified disk preparation. Radiolabeled sodium ion ($^{22}Na^+$) transport was measured as follows. $^{22}Na^+$ was preloaded into the disks by exposure to extravesicular radioisotopically labeled cation, followed by replacement of the extravesicular labeled pool with an unlabeled pool of the same cation concentration (60 mM in Na). This procedure creates a transmembrane $^{22}Na^+$ gradient but maintains equilibrium between intravesicular and extravesicular Na^+ concentrations during exposure of the disks to cyclic nucleotide.

Relative to cGMP, 8-Br-cGMP is a poor substrate for hydrolysis by the ROS cyclic nucleotide phosphodiesterase (Zimmerman et al., 1986); thus, concentration changes and proton gradient generation during its exposure to the disks are minimized. For this reason, the release of cations activated by 8-Br-cGMP was most extensively characterized in this study. A complete description of the kinetics of decay of $^{22}Na^+$ release necessitated performing parallel experiments on three different time scales (Figure 3) due to methodological constraints imposed by the rapid superfusion system (see Experimental Procedures for further details). The release of $^{22}Na^+$ stimulated by continuous superfusion with near-saturating levels of 8-Br-cGMP (25 μM) is transient in character: when the $^{22}Na^+$ release event is measured by collection of superfusate at 25-ms intervals (Figure 3), maximal activation of $^{22}Na^+$ efflux reproducibly occurs within 25 ms of introduction of the nucleotide, i.e., as rapidly as can be measured. The response immediately begins to decay and is severalfold lower within a few hundred milliseconds of introduction of 8-Br-cGMP. As shown, the decay of this transient response can be precisely fitted to the sum of two exponential decay processes:

$$R = Ae^{-t/p} + Be^{-t/q} \quad (1)$$

where R is the $^{22}Na^+$ release rate at any time (t) after the response is maximally activated, A and B are the relative amplitudes of two separately decaying release processes, and

p and q are the time constants of, respectively, the faster and slower of the two decaying processes.

The time constants that best fit the data of Figure 3B (50-ms collection intervals) are p = 0.2 s and q = 1.6 s (F value, 4540). Double-exponential decay processes with the same two time constants also closely fit the data for 8-Br-cGMP-stimulated $^{22}Na^+$ release monitored at 25-ms intervals (Figure 3A), as well as the response measured at 0.5-ms intervals during 8 s of exposure to 8-Br-cGMP (Figure 3C). Other equations did not fit this decay data with the precision of the double-exponential model; these include a single-exponential decay process (Figure 3B, F value of 1270) and polynomial functions of up to the fifth degree (F value of 3510).

The kinetics and magnitude of $^{22}Na^+$ efflux stimulated by 100 μM cGMP closely resemble the response to 8-Br-cGMP described above, as documented later (Figure 8). When preloaded into the purified disks by exchange from an extravesicular isotope pool as in the $^{22}Na^+$ experiments, $^{134}Cs^+$ efflux was also stimulated by cyclic guanosine nucleotides (data not shown). The observed kinetics resembled those of $^{22}Na^+$ release.

The Ca^{2+} efflux activity observed here occurs in the total absence of extravesicular ATP and at mean free intravesicular ATP levels which do not exceed 4 μM (R. Barnes, unpublished data).

Time Resolution of the Superfusion Method. Measurement of the time course of the decay of 8-Br-cGMP-stimulated $^{22}Na^+$ release is not limited by the time resolution of the superfusion method. Information on the mixing time of the superfusion system was obtained by studying the introduction and washout of ^3H_2O. These results indicate that mixing exhibits single-exponential kinetics and is 90–95% complete within 30 ms (data not shown). The fit to the data for wash-in and washout provides time constants of 10.9 and 13.8 ms, respectively, indicating that the introduction and removal of ^3H_2O follow very similar time courses.

However, the kinetics of exposure of cyclic nucleotide to its receptors at the disk membrane may not entirely reflect the mixing kinetics of the superfusion chamber per se: it is conceivable that some of the disks are in regions of the filter in the superfusion chamber that are more stagnant, or that the deposition of disk vesicles on the filter creates a barrier that prevents rapid washout of released $^{22}Na^+$. To deal with this concern, the efficiency of superfusion was evaluated by examining the rate and extent of ionophore-evoked release of $^{22}Na^+$ (Figure 4). The ionophore monensin (25 μM), which can generate net electroneutral exchange of $^{22}Na^+$ with other monovalent cations (Antonenko & Iagushinski, 1983), is rapidly incorporated into the membrane—the $^{22}Na^+$ efflux rate was maximal within 25–30 ms of exposure of the ionophore to the disks (Figure 4A). Monensin releases greater than 90% of intravesicular $^{22}Na^+$ within 190 ms (Figure 4B). These results indicate that nearly all of the disks are exposed to the superfusion medium. Approximately 1% of the radiolabel remains nonspecifically bound to the filter; the remaining 4% of the radiolabel that does not leave the superfusion chamber may reflect a small fractions of disks that are not superfused or may be accounted for by $^{22}Na^+$ remaining bound to external disk membrane sites.

The decay of monensin-stimulated $^{22}Na^+$ release is substantially faster than the observed rate of decay of 8-Br-cGMP-stimulated $^{22}Na^+$ efflux. The time course of decay of the rate of monensin-evoked efflux of $^{22}Na^+$ from this maximum was found to fit single-exponential kinetics with a time

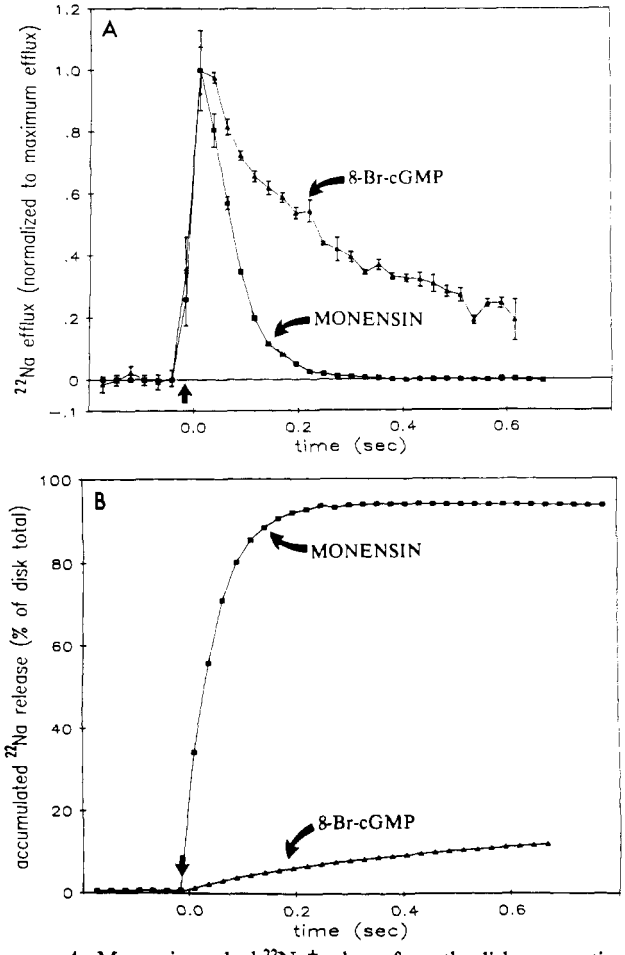

FIGURE 4: Monensin-evoked $^{22}Na^+$ release from the disk preparation. Panel A displays the comparative time course of the responses to monensin (■) and 25 μM 8-Br-cGMP cGMP (▲) normalized so that the maximum rate of release in each case = 1. Panel B displays the total accumulated $^{22}Na^+$ release induced by monensin (■) or 8-Br-cGMP (▲) up to the indicated time. The total accumulated release generated after 600 ms of exposure was 94.2% of incorporated counts by monensin, and 11.9% of incorporated counts by 8-Br-cGMP. The disks were initially superfused with standard buffer. At the point indicated by the vertical arrow in each panel, delivery of 50 μM monensin (■) or 25 μM 8-Br-cGMP (▲) in standard buffer was initiated by a valve gating switch from the "buffer" reservoir to the "drug" reservoir. Fractions were collected at 26-ms intervals. For the monensin observations, each data point is the mean of three experiments (the average SEM was 13.6% of the radioactivity in each fraction). For the 8-Br-cGMP data, the mean was of four runs, and the average SEM was 6.0% of the released radioactivity.

constant of 71 ms (Figure 4A). The kinetics of monensin-evoked $^{22}Na^+$ efflux provide a *minimum* estimate of the rate at which radiolabel can be exchanged out of disks trapped on filters within this superfusion system, thus demonstrating that the superfusion system can resolve the decay of cyclic nucleotide stimulated $^{22}Na^+$ efflux on a more rapid time scale than the rate of decay actually observed. Thus, the calculated biphasic decay constants for 8-Br-cGMP-stimulated $^{22}Na^+$ release are, primarily, intrinsic parameters reflecting the movement of ions across the disk membrane and are not attributable to limitations imposed by this superfusion method.

Decay of 8-Br-cGMP-Stimulated $^{22}Na^+$ Efflux Is Not Due to Depletion of Releasable $^{22}Na^+$. A possible explanation for the transient nature of monovalent cation release from the purified disk preparation is that activation of the disk-associated ion channels by 8-Br-cGMP rapidly depletes the releaseable pool of $^{22}Na^+$, that is only a small fraction of the total ionophore-dischargeable pool (see Figure 4B). The biphasic nature of the decay process could reflect heterogeneity

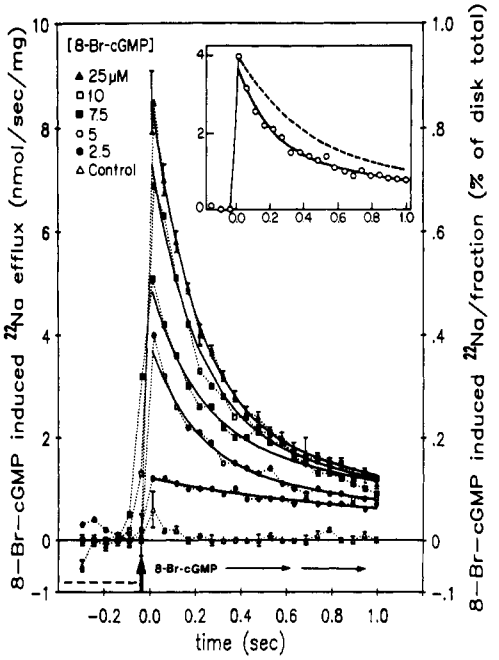

FIGURE 5: Concentration dependence of 8-Br-cGMP-induced $^{22}Na^+$ influx from the purified disk preparation. Disks were preloaded with $^{22}Na^+$ and superfused with standard buffer. The vertical arrow denotes the point of immediate switch to continuous superfusion with 8-Br-cGMP, at concentrations (note descending amplitudes) of 25 (▲), 10 (□), 7.5 (■), 5 (○), 2.5 (●), or 0 μM (△). Fractions were collected continuously at 53-ms intervals. The data for each [8-Br-cGMP] tested are connected by dotted lines. The solid curves for each [8-Br-cGMP](—) represent the fit of the data to biphasic exponential decay kinetics (eq 1) with p = 0.2 s and q = 1.2 s. The dashed curve of the inset (- - - -) represents the fit of the decay kinetics of the release event observed at 5 μM 8-Br-cGMP (○) to a model attributing the decay of release as solely a consequence of depletion of a pool of releasable $^{22}Na^+$, using the equation $J_{5\mu M} = A_{25\mu M}De^{-tD/0.2} + B_{25}De^{-tD/1.6}$ where D = the ratio of the initial amplitude of ^{22}Na release observed at 5 μM 8-Br-cGMP to that observed at 25 μM [8-Br-cGMP] (see text for the basis of this equation). The *solid curve of the inset* represents, again, the best fit of the data to biphasic exponential kinetics (*for comparison*). The scalar value of $^{22}Na^+$ efflux denoted by the dashed horizontal lines (lower left) represents the basal level of $^{22}Na^+$ efflux prior to stimulation with 8-Br-cGMP. Each data symbol denotes the means of three separate experiments. For clarity, the SEM denoted by the vertical bars, is illustrated only for the maximum and minimum [8-Br-cGMP]. For the other concentrations tested, the average SEM as a percentage of the value of each data point, was 7.4% for 10 μM, 10.9% for 7.5 μM, 15.7% for 5 μM, 7.8% for 2.5 μM, and 6.0% for 0 μM. See Experimental Procedures for additional details.

in the morphology (e.g., intravesicular aqueous compartment) of the R-band disk preparation and/or contamination of the disks with membrane vesicles of nondisk origin. This model would predict that if $^{22}Na^+$ release were stimulated by concentrations of 8-Br-cGMP which produce lower levels of channel activation, the decay constants ("p" and "q") would be proportionately larger because it would take longer for the releasable pool(s) of $^{22}Na^+$ to be depleted.

An alternative basis for this decay is that an intrinsic mechanism exists for closure or inactivation of the disk-associated cation channels. The time course and rate of $^{22}Na^+$ efflux, as a function of 8-Br-cGMP concentration (Figure 5), provide evidence for an intrinsic inactivation process rather than cation gradient depletion. The data throughout this concentration range are closely fit by biphasic decay kinetics with the same decay constants derived for the response to near-saturating levels of 8-Br-cGMP. The cation gradient depletion model would predict, for example, that at 5 μM 8-Br-cGMP, where the observed initial amplitude of 8-Br-cGMP-stimulated $^{22}Na^+$ release is more than 2-fold lower than

Table I: Time Constants for Decay of $^{22}Na^+$ Efflux: Results of the Best Fit to Biphasic Exponential Decay Kinetics

[8-Br-cGMP] (μM)	fraction collection interval (ms)	fast decay (s ± SE)[c]	slow decay (s ± SE)[c]
25 (2)[a]	500	0.23 ± 0.01	1.61 ± 0.08
25 (7)	52.6	0.20 ± 0.04	1.67 ± 0.48
10 (4)	52.6	0.18 ± 0.06	1.63 ± 0.34
7.5 (6)	52.6	0.07 ± 0.02	0.83 ± 0.11
5 (5)	52.6	0.19 ± 0.09	1.16 ± 0.68
2.5 (4)	52.6	*b*	1.02 ± 0.12
1 (3)	52.6	*b*	1.20 ± 0.16

[a] Number of experiments. Combined data from two ROS disk preparations. [b] Fit best to a single exponential. [c] SE is the standard error for the best fit of each time constant to the data for decay of 8-Br-cGMP-stimulated $^{22}Na^+$ efflux. For data collected at 500 ms intervals (first row), the decay was monitored for 7 s following maximal activation; for the rest of the data, decay was monitored for 1 s following activation.

Table II: Effect of *l-cis*-Diltiazem on $^{22}Na^+$ Efflux

nucleotide	decay phase	amplitude of initial efflux[a] control	amplitude of initial efflux[a] *l-cis*-diltiazem[c]	% of control[b]
8-Br-cGMP (15 μM)	slow	2.2 ± 0.6	0.5 ± 0.1	23
	fast	5.3 ± 0.6	3.0 ± 0.2	57
cGMP (100 μM)	slow	3.0 ± 0.8	1.0 ± 0.1	33
	fast	9.4 ± 0.8	6.0 ± 0.3	64

[a] Nanomoles of $^{22}Na^+$ per second per milligram of protein. [b] ([*l-cis*-diltiazem]/[control]) × 100. [c] 25 μM *l-cis*-diltiazem in all buffers. Disk membranes (10 μL of 8 mg of protein/mL) were incubated with 25 μM *l-cis*-diltiazem and with $^{22}Na^+$ (200 μCi of $^{22}Na^+$ in 60 mM NaCl) for 4 h, 0 °C, prior to superfusion. The data analyzed are displayed in Figure 7. The error band shown is ± the standard error of the best fit of each amplitude term to the data for the decay of the $^{22}Na^+$ efflux during the first second following nucleotide activation.

that observed at 25 μM 8-Br-cGMP, one would concomitantly observe >2-fold longer decay constants. As illustrated (Figure 5), this prediction does not fit the data: rather than increasing as [8-Br-cGMP] is reduced, the decay constants p and q which *best* fit each concentration tested (Table I) remain essentially fixed or actually decrease somewhat (the decrease is of borderline statistical significance).

Differential Sensitivity of the Two Components of Release to Activation and Inhibition. The maximum initial rate of $^{22}Na^+$ efflux is the sum of the amplitudes (termed "*A*" and "*B*" in eq 1) of each of the two separate, independently decaying responses to 8-Br-cGMP activation. A plot of the amplitudes of each of the rapidly ("*A*") and more slowly decaying ("*B*") responses as a function of [8-Br-cGMP] (Figure 6) demonstrates differences in their sensitivity to the nucleotide. The concentration dependency for 8-Br-cGMP activation of the slowly decaying process is homologous to simple Michaelis–Menten saturation kinetics (apparent Hill coefficient of 1.0), whereas the corresponding relationship for the rapidly decaying process is sigmoidal in character (apparent Hill coefficient of 2.1). The [8-Br-cGMP] required for half-maximal activation of the slower phase is severalfold lower than that required for activation of the rapid phase (EC_{50} of 2.8 and 8.4 μM, respectively).

l-cis-Diltiazem has been shown to block cGMP-stimulated channels in excised patches of ROS plasma membrane (Stern et al., 1986) and blocks cGMP-stimulated $^{45}Ca^{2+}$ release from ROS membrane vesicles (Koch & Kaupp, 1985). *l-cis*-Diltiazem blocks cyclic nucleotide activation of transient $^{22}Na^+$ release: at the drug concentration (25 μM) that corresponds to the IC_{50} for blockade of the overall response to 8-Br-cGMP,

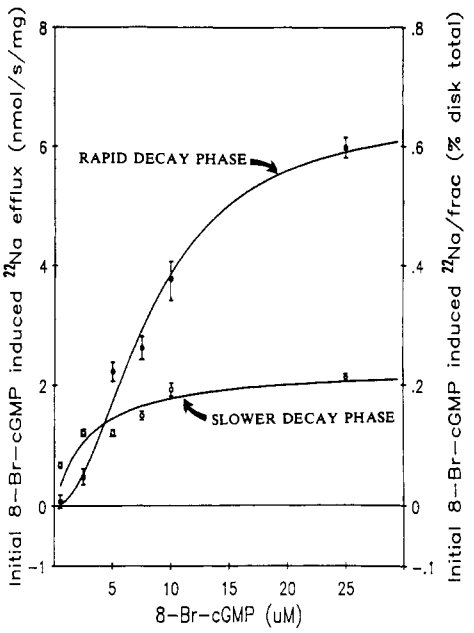

FIGURE 6: Concentration dependence for 8-Br-cGMP activation of the rapid decay (●, p = 0.2 s) and slower decay (○, q = 1.6 s) phases of $^{22}Na^+$ efflux from the purified disk preparation. The initial amplitude of the $^{22}Na^+$ efflux event observed at each [8-Br-cGMP] tested was treated as the sum of the amplitudes ("A" and "B") of two separately decaying responses, as described in eq 1 (see text). The two amplitude terms were each derived from curve-fitting analysis of the initial second of 8-Br-cGMP-induced ^{22}Na efflux at each [8-Br-cGMP] tested (cf. Figure 4). The derived A (●) and B (○) terms are plotted as a function of [8-Br-cGMP]; the vertical bars denote standard errors for the fit of each of the two amplitude terms to the ^{22}Na efflux data. The curve used to fit the data for the rapidly decaying phase was the best fit to the second-order Hill equation [c.f. Stryer (1981)] of the form $A/A_{max} = [8\text{-Br-cGMP}]^2/\{(EC_{50})^2 + [8\text{-Br-cGMP}]^2\}$ where A/A_{max} is the ratio of the amplitude of the rapid decay phase of release observed at a given [8-Br-cGMP] to the maximum amplitude observed at saturating [8-Br-cGMP] and EC_{50} is the [8-Br-cGMP] producing half-maximal amplitude of the rapid decay phase (determined to be 8.4 μM). The curve used to fit the data for the slower decay phase was the best fit to Michaelis–Menten saturation kinetics for activation of the response (apparent $K_m = EC_{50}$ = 2.9 μM). The number of experiments at each [8-Br-cGMP] concentration are the following: 25 μM, 7; 10 μM, 4; 7.5 μM, 6; 5 μM, 5; 2.5 μM, 4; and 1 μM, 3.

the slow decay phase is relatively more sensitive than the rapid decay phase to inhibition by the drug (Table II and Figure 7A). The kinetics and the amplitude of the response to near-saturating levels of cGMP (100 μM) were comparable to those observed for the 8-Br-cGMP response (Table II and Figure 7B). As shown, *l-cis* diltiazem blocks the response to cGMP; the IC_{50} levels and selectivity for the slow decay phase are similar to its inhibition of the 8-Br-cGMP response.

8-Br-cGMP-Stimulated Release of Actively Accumulated $^{45}Ca^{2+}$ Exhibits Similar Biphasic Decay Kinetics. Purified disks were actively loaded with $^{45}Ca^{2+}$ by ATP-driven Ca uptake as previously described (Puckett & Goldin, 1986) but in the absence of phosphate ion (a known Ca^{2+} chelator). Under these conditions, the level of ATP-dependent Ca^{2+} uptake is severalfold lower than that obtained in the presence of phosphate (mean values of 1.3 vs 5.8 nmol/mg of disk protein). In the absence of Na^+, 8-Br-cGMP (25 μM) stimulates release of actively accumulated $^{45}Ca^{2+}$. As resolved on the 100-ms time scale, the release event closely resembles the transient $^{22}Na^+$ efflux in its kinetics of activation and decay (Figure 8). The biphasic decay constants ("p" and "q") that best fit the data are 0.15 and 1.3 s, respectively. The rapidly decaying phase comprises most (65%) of the initial amplitude of the response, in good agreement with the relative amplitudes

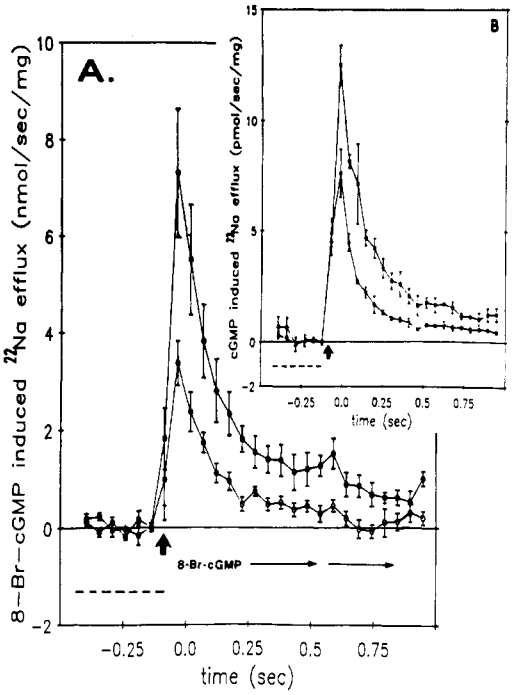

FIGURE 7: Inhibition by *l-cis*-diltiazem of 8-Br-cGMP- and cGMP-induced $^{22}Na^+$ efflux from the purified disk preparation. Identical samples of disk membranes (10 μL of 8 mg of protein/mL) were incubated either with or without 25 μM *l-cis*-diltiazem and in the presence of $^{22}Na^+$ prior to superfusion. *l-cis*-diltiazem (25 μM) was included in all superfusion buffers both prior to and subsequent to introduction of the nucleotide. All other details were as described under Experimental Procedures and in the legends of Figures 1 and 4. The switch to cyclic nucleotide is indicated by the vertical arrow; superfusate fractions were collected at 53-ms intervals. The scalar value of $^{22}Na^+$ efflux denoted by the dashed horizontal lines (lower left of panels A and B) represents the basal level of $^{22}Na^+$ efflux prior to stimulation with 8-Br-cGMP. Panel A: (●) 15 μM 8-Br-cGMP (n = 4); (○) 15 μM 8-Br-cGMP + 25 μM *l-cis*-diltiazem (n = 8). Panel B (inset): (●) 100 μM cGMP (n = 2); (○) 100 μM cGMP + 25 μM *l-cis*-diltiazem (n = 2).

of the two phases of 8-Br-cGMP-stimulated $^{22}Na^+$ efflux (see Figures 6 and 7).

As an alternative to active loading of $^{45}Ca^{2+}$ via the ATP-dependent Ca^{2+} pump, passive equilibration of the disk preparation with $^{45}Ca^{2+}$ in the absence of ATP generated a pool of intracellular Ca^{2+} that was the source of release by 8-Br-cGMP (Figure 9). The kinetics of the transient $^{45}Ca^{2+}$ release event, observed after removal of extravesicular Ca^{2+}, were similar to those observed for 8-Br-cGMP-stimulated release of actively accumulated $^{45}Ca^{2+}$. A response of comparable amplitude was only observed when the preparation was equilibrated with at least 2 mM external $^{45}Ca^{2+}$. Equilibration with 5 mM $^{45}Ca^{2+}$ resulted in a response severalfold higher in amplitude than observed for release of actively accumulated $^{45}Ca^{2+}$. The biphasic exponential decay constants of p = 0.2 s and q = 1.6 s accurately fit the data throughout a broad range of external [Ca^{2+}] (1–5 mM) used for passive equilibration. The *relative* amplitudes of the rapid and slow decaying responses were comparable to that observed for 8-Br-cGMP-stimulated release of actively accumulated $^{45}Ca^{2+}$.

Selective Inhibition of the Rapidly Decaying Phase of $^{45}Ca^{2+}$ Release by Na^+. Extravesicular Na^+ inhibits 8-Br-cGMP-stimulated release of actively accumulated $^{45}Ca^{2+}$ with a relatively steep concentration dependence (Figure 8): the [Na] for half-maximal reduction of the initial amplitude of $^{45}Ca^{2+}$ efflux occurs, and Na^+ selectively inhibits the rapidly decaying phase of the response. As quantitated by curve-fitting

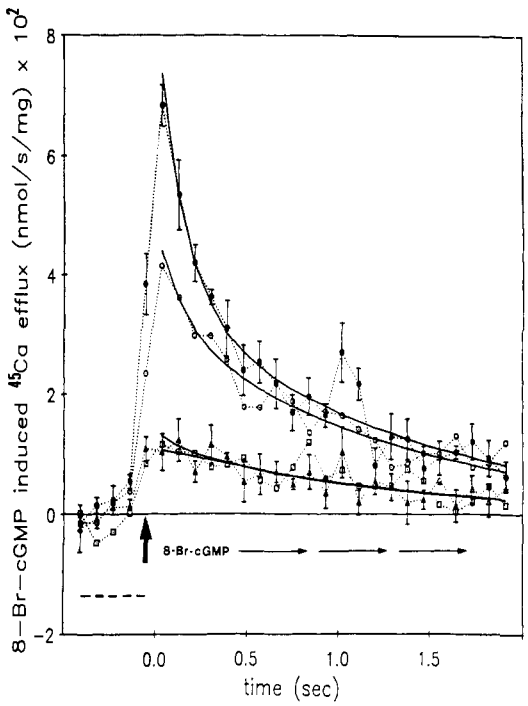

FIGURE 8: 8-Br-cGMP-stimulated $^{45}Ca^{2+}$ release from the purified disk vesicles. The vesicles were actively loaded in phosphate-free buffer with $^{45}Ca^{2+}$ via the associated ATP-dependent uptake system. Stimulation of $^{45}Ca^{2+}$ from the vesicles by continuous superfusion with 25 μM 8-Br-cGMP was performed by a protocol similar to that of the $^{22}Na^+$ experiments (Figure 3), but phosphate-free (MOPS) buffers were employed. Aliquots of the vesicles were preequilibrated and continuously superfused with buffer containing varying $[Na^+]$: 0 mM (●); 10 mM (○); 20 mM (△); and 40 mM (□). All solutions employed contained the same $[Na^+]$ initially used for disk vesicle equilibration. Superfusate fractions were continuously collected at 94-ms intervals. The solid curves denote the best fit of the decay of the response to biphasic exponential decay kinetics (eq 1 of text), with decay constants $p = 0.15$ s and $q = 1.3$ s; those decay constants were determined from the best fit of the data obtained in Na^+-free medium. Each data symbol is the mean of three seprate experiments. For visual clarity, error bars are displayed only for the experiments performed in 0 and 40 mM $[Na^+]$ but were typical of the other sets of experiments. The scalar value of $^{22}Na^+$ efflux denoted by the dashed horizontal lines (lower left) represents the basal level of $^{22}Na^+$ efflux prior to stimulation with 8-Br-cGMP.

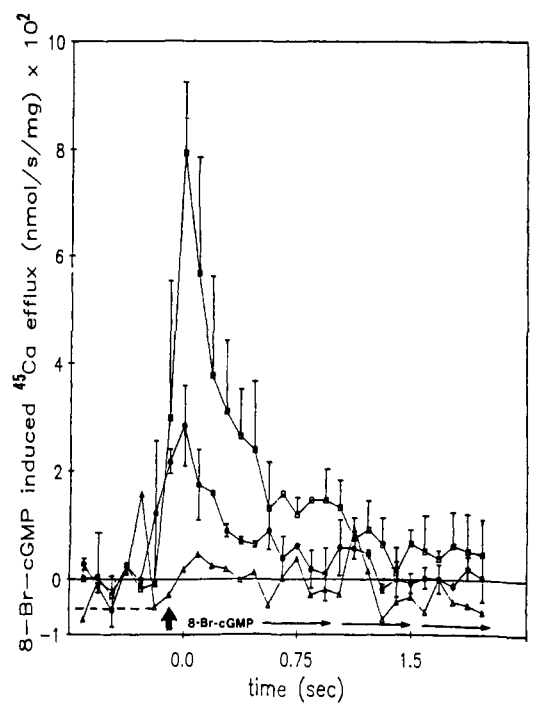

FIGURE 9: Amiloride block of 8-Br-cGMP-stimulated release of actively accumulated $^{45}Ca^{2+}$. The $^{45}Ca^{2+}$ release experiments were performed in duplicate under Na^+-free conditions as in Figure 9, but with the disk vesicles preincubated for 30 min, 24 °C, in 0 (□), 30 (○), or 300 μM (△) amiloride. The same [amiloride] was maintained in the buffer and 8-Br-cGMP reservoirs for each corresponding set of experiments. The vertical arrow denotes initiation of superfusion with 25 μM 8-Br-cGMP. The scalar value of $^{22}Na^+$ efflux denoted by the dashed horizontal lines (lower left) represents the basal level of $^{22}Na^+$ efflux prior to stimulation with 8-Br-cGMP.

analysis (eq 1, $p = 0.15$ s and $q = 1.3$ s), and 5–10 mM Na^+ ~60% of the rapid decay phase of the response is abolished, with little or no reduction in amplitude of the slower decay phase. At Na^+ concentrations at or above 20 mM, the rapid decay phase is virtually eliminated, but the amplitude of the slower decay phase exceeds 50% of the control value. The level of ATP-dependent incorporation of $^{45}Ca^{2+}$ was not significantly affected by removal of Na^+ prior to the incubation (data not shown); this indicates that the inhibition by Na^+ of $^{45}Ca^{2+}$ release was not secondary to blockade of the ATP-dependent Ca^{2+} uptake activity which generated the 8-Br-cGMP-releasable $^{45}Ca^{2+}$ pool.

Amiloride inhibits a variety of membrane ion transport activities including Na^+/Ca^{2+} exchange in heart (Siegl et al., 1984) and brain (Kaczorowski, 1985); the light-sensitive current in amphibians (Fain & Lisman, 1981) is reportedly insensitive to amiloride but is blocked by an amiloride derivative, 3′,4′-dichlorobenzamil (Nicol et al., 1987). Amiloride blocks 8-Br-cGMP-stimulated $^{45}Ca^{2+}$ release from the purified disk vesicles with an IC_{50} of ~30 μM (Figure 10). The inhibition occurs in the absence of Na^+, consistent with a direct interaction of this drug with the ion channel rather than an indirect consequence of inhibition of Na^+/Ca^{2+} exchange. Amiloride did not display substantial selectivity for inhibition

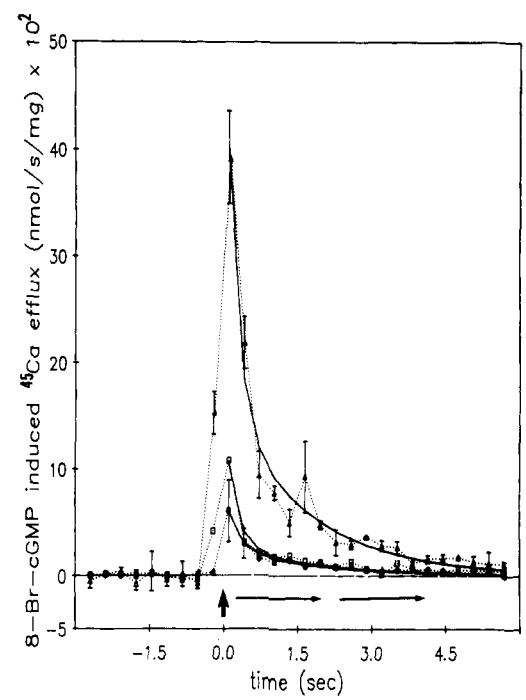

FIGURE 10: Stimulation by 8-Br-cGMP of release of $^{45}Ca^{2+}$ preloaded into disks by passive equilibration. Release of $^{45}Ca^{2+}$ was measured in Na-free medium as in Figure 9, but with the following differences: $^{45}Ca^{2+}$ [1 (○), 2 (□), or 5 mM (▲)] was preloaded into the disk vesicles by passive equilibration (overnight at 0 °C). Extravesicular Ca was subsequently removed. The solid curves demonstrate the best fit of the decay of the $^{45}Ca^{2+}$ release to biphasic kinetics, with $p = 0.2$ s and $q = 1.6$ s. Each data point is the average of duplicate experiments.

of either of the two components of the response. The 8-Br-cGMP-stimulated $^{45}Ca^{2+}$ release was also inhibited by *l-cis-*

diltiazem (data not shown) in a manner similar to that described above for $^{22}Na^+$ release.

Discussion

Experimental Conditions and Interpretation of Flux Measurements. The $^{22}Na^+$ efflux experiments were designed to produce quantitative kinetic measurements of cyclic nucleotide induced increases in Na^+ permeability: thus, they wre performed in the absence of concentration gradients or osmotic gradients. Since the fluxes that are observed presumably occur in the absence of a membrane potential or electrochemical driving force on Na^+ movement, no net transmembrane movement of Na^+ should occur during the experiments. In contrast, the 8-Br-cGMP-induced $^{45}Ca^{2+}$ efflux was observed under conditions in which an outward-directed Ca^{2+} concentration gradient was experimentally created, either by active ATP-dependent $^{45}Ca^{2+}$ accumulation or (in parallel experiments) by passive equilibration of $^{45}Ca^{2+}$ with the vesicles, followed in both cases by the removal of extravesicular Ca^{2+}. These conditions were established to mimic those under which cGMP-stimulated *net* Ca^{2+} efflux from disks may be hypothesized to occur in ROS in vivo. Despite these experimental differences, the 8-Br-cGMP-stimulated effluxes of $^{22}Na^+$ and $^{45}Ca^{2+}$ were nearly identical kinetically.

Rapid 8-Br-cGMP Activation of Cation Flux by Direct Chemical Excitation of Ion Channels. The results reported here demonstrate maximal activation of cation flux within 25 ms following introduction of extravesicular 8-Br-cGMP. The Ca^{2+} channel activity observed here occurs in the total absence of extravesicular ATP and at free intravesicular ATP levels below 4 μM (R. Barnes, unpublished data). Thus, a phosphokinase-mediated mechanism of channel activation is unlikely, since (a) phosphokinase-mediated regulatory events previously studied under physiological conditions occur after a longer delay following elevation of cyclic nucleotide levels, and (b) physiological intracellular levels of the kinase substrate, ATP, are millimolar, far greater than those observed here. This indicates a mechanism of channel activation by direct interaction of cGMP with the channel-containing membrane protein complex. Such a mechanism is consistent with and predicted by prior observations (Caretta & Cavagioni, 1983; Fesenko et al., 1985).

What is more unexpected is the subsequent time course and certain quantitative aspects of the pharmacology of the transient cGMP-stimulated cation gating event, as first characterized on such a rapid time scale in a disk preparation. Activation of cation efflux by 8-Br-cGMP is immediately followed by its biphasic exponential decay over the next few seconds. The values of the decay time constants [*which we could not resolve using our prior crude experimental device (Puckett & Goldin, 1986)*] are observed here to be independent of whether a monovalent cation (Na^+) or bivalent cation (Ca^{2+}) is the species gated. As previously hypothesized (Puckett & Goldin, 1986), both phases of the decay are produced by a process resulting in *conductance inactivation* (as opposed to radioisotopic ion gradient depletion). This conclusion is based on the observation that the decay time constants are not increased at concentrations of 8-Br-cGMP that stimulate submaximal rates of cation efflux, as compared with the decay at saturating [8-Br-cGMP]. A corrolary of this is the observation that the *total* amount of 8-Br-cGMP-stimulated radioisotope release observed before decay is complete is lower rather than the same at submaximal versus saturating [8-Br-cGMP].

The mechanism of this inactivation phenomenon is undefined. Mechanisms similar to those responsible for agonist-induced desensitization (Neubig et al., 1982) and/or deactivation (Boyd, 1987) of the ion channel gated by nicotinic acetylcholine receptors may at least in part explain these observations. Acetylcholine receptor desensitization is reversed simply by removing the agonist for a sufficient period of time before its reintroduction, while deactivation is a more irreversible process that is incompletely understood.

Evidence That the Observed cGMP-Stimulated Cation Transport Activity Is Disk-Associated. The strongest argument that the Ca^{2+} release is occurring from ROS disks (or a subset of the disk population) is based on the finding that the intravesicular pool of $^{45}Ca^{2+}$ that is outwardly gated by 8-Br-cGMP can be formed by active accumulation via an ATP-dependent Ca^{2+} uptake activity associated with this disk preparation. This Ca^{2+} uptake activity copurifies with disks and pumps Ca^{2+} into the disk lumen, on the basis of the following previously described evidence (Puckett et al., 1985). (a) The Ca^{2+} uptake activity always precisely comigated with the disks as a well-resolved band (termed the "R-band") in several density gradient systems of differing osmotic and ionic strengths; this is unlikely to be a mere coincidence because the unusual osmotic properties of sealed disks cause characteristic variations in their density gradient sedimentation behavior as a function of the osmolarity of the gradient solutions. (b) The level of ATP-dependent Ca^{2+} uptake activity in the disk preparation is relatively consistent with estimates of Ca^{2+} sequestration capacity within vertebrate ROS (Szuts & Cone, 1977; Hagins & Yoshikami, 1975).

The present study shows that the amplitude of 8-Br-cGMP-stimulated release of *actively accumulated* $^{45}Ca^{2+}$ is comparable to the amplitude of release of $^{45}Ca^{2+}$ *passively equilibrated* with the disk preparation, but only when the external [Ca^{2+}] employed for passive equilibration is at least 2 mM. This corroborates the previous estimate (Puckett et al., 1985) that the ATP-dependent Ca^{2+} uptake activity can generate steady-state Ca^{2+} levels of several millimolar within the disks, which is what is expected on the basis of the above cited estimates of the exchangeable [Ca^{2+}] in disks in vivo. It also suggests that the *maximum naturally occurring* rate of cGMP-stimulated Ca^{2+} release in native ROS (not yet measured) may turn out to be similar to that observed in the R-band disk preparation.

The fast time resolution of the superfusion method currently employed enabled more accurate, direct measurement of the *initial* rate of 8-Br-cGMP-stimulated Ca^{2+} release. If Ca^{2+} release could be measured on an even more rapid time scale, e.g., a millisecond rather than the 25-ms resolution achieved here, it is possible that the maximal release rate would be even larger than given here. In any case, the peak rate of 8-Br-cGMP-stimulated release of actively accumulated ^{45}Ca observed here [as high as 8 nmol (mg of protein)$^{-1}$ min^{-1}] is nearly an order of magnitude larger than our previous observations (Puckett & Goldin, 1986), which were made on a much slower time scale and could not resolve the true initial rate or time course of release. On the basis of the same estimates of the dimensions and morphology of bovine disks and ROS employed in that previous study, this release rate translates to $\sim 10^4$ Ca^{2+} per disk per second. Such a rate of Ca^{2+} release is sufficient in principle to produce a 1 μM change in cytoplasmic [Ca^{2+}] within <20 ms; maximum release rates this high are of sufficient duration to substantially alter ROS cytoplasmic free Ca concentrations, which current measurement techniques demonstrate to be submicromolar (McNaughton, 1986; Miller & Korenbrot, 1986).

Evidence for Multiple Classes of cGMP-Stimulated Channels in the Disk Preparation. The two phases of decay are differentially sensitive to activation by 8-Br-cGMP, to block by *l-cis*-diltiazem, and to inhibition by Na. This defines the existence of two functionally distinct forms of cGMP-stimulated channel that differ in their kinetics of decay, pharmacological properties, and sensitivity to the ionic environment. The issue of whether these distinct forms represent different channel protein molecules or different functional states of the same molecule is unresolved at present. The criteria used to identify these channel subclasses are somewhat analogous to the electrophysiological criteria employed to identify the "T", "L", and "N" subclasses of voltage-sensitive Ca channels in nerve (Nowycky et al., 1985) and cardiac (Nilius et al., 1985) cells: these distinct subclasses were resolved on the basis of their voltage dependence for activation, kinetics of inactivation, and differential sensitivity to channel blocking agents.

Evidence from other laboratories has previously raised the issue of possible heterogeneity of cGMP-sensitive channels in ROS. Although *l-cis*-diltiazem inhibits cGMP-stimulated Ca^{2+} efflux from ROS membrane vesicles (Koch & Kaupp, 1985) and the channel of patch-clamped ROS plasma membranes (Stern et al., 1986), it is ineffective in blocking the photocurrent when perfused into intact rod cells (Stern et al., 1986). Cook et al. (1987) and Matesic and Liebman (1987) have separately reported the purification and reconstitution of cGMP-activated channels from bovine ROS. In addition to differences in the molecular weights for the major components of their preparations, the preparation of Cook et al. exhibits a high degree of cooperativity in cGMP activation (n_H ~3.1) and low *l-cis*-diltiazem sensitivity, while Matesic and Liebman report less cooperativity (n_H ~1.7) and inhibition by *l-cis*-diltiazem.

Koch and Kaupp (1985) reported two kinetic components of cGMP-stimulated Ca^{2+} efflux from ROS membrane vesicles; while our paper was in preparation, differential Na^+ and *l-cis*-diltiazem sensitivity of those two kinetic components was reported (Schnetkamp, 1987). The relationship between the observations of Schnetkamp and ours is significant but not completely clear: in the former studies, the more rapid component terminated within several seconds, whereas the slower component persisted for several minutes. In contrast, *both* components of the response we observe in the purified disk vesicle preparation and characterize here on a much more rapid time scale terminate within seconds.

Properties of the cGMP-Stimulated Cation Transport Activity in Relation to the cGMP-Stimulated Ion Channels of Patch-Clamped Plasma Membranes. Our measurements of maximum cation efflux rates are a *lower* limit for the real value, as it is possible that we are not measuring the true initial rates of cation movement. With this qualification, it is nonetheless useful to point out some relationship between our observations and direct electrophysiological measurements of ROS plasma membrane channels made by others. The following assumes, not unreasonably, that our maximum efflux rates approximate peak levels of ion channel activity in the disk preparation.

Our measurement of the peak amplitude of $^{22}Na^+$ efflux [~10 nmol s^{-1} (mg of disk protein)$^{-1}$] observed in *60 mM* Na^+ upon channel activation by near-saturating [8-Br-cGMP] or [cGMP] is 25-fold higher than the peak amplitude of 8-Br-cGMP-stimulated ^{45}Ca efflux (0.4 nmol s^{-1} mg^{-1}) observed in the absence of Na after the disk vesicle preparation is equilibrated with *5 mM* $^{45}Ca^{2+}$. Taking into account the experimental difference in the concentrations of Ca^{2+} and Na^+, this translates to an overall channel selectivity ratio for Ca:Na of ~0.5. Because the relative proportions of the rapid and slower decaying phases in the total response are similar for both $^{22}Na^+$ and $^{45}Ca^{2+}$ release, both components of the response clearly exhibit a similar low degree of selectivity between Na and Ca, as in the case for amphibian ROS plasma membrane channels (Hodgkin et al., 1985; Furman & Tanaka, 1987).

The most striking kinetic difference between the current study and the behavior of ROS plasma membrane channels under patch-clamp conditions (Fesenko, 1985; Haynes et al., 1986; Zimmerman & Baylor, 1986) is that the activity of patch-clamped channels does not exhibit the decay noted for both components of the cGMP-stimulated ion conductance characterized here. This could be attributable to differences in experimental conditions, differences in the behavior of the putative disk-associated channels due to environmental or regulatory factors not found in the plasma membrane, or intrinsic molecular differences in the classes of channels.

Approximating a bovine disk as 1 μm in diameter (Fein & Szuts, 1982) containing 10^5 rhodopsin molecules (Amis et al., 1981), and given the observation that at least 60% of the protein in the R-band disk preparation is rhodopsin of M_r ~40 000 (Puckett et al., 1985), the area of membrane per milligram of protein in this preparation is ~1.4×10^3 cm^2. The calculated cGMP-stimulated ^{22}Na flux per unit membrane area defines an average P_{Na} of ~1.2×10^{-7} cm/s, substantially lower than corresponding values for patch-clamped ROS plasma membranes.

Possible Significance of Modulation by Na^+ of 8-Br-cGMP-Stimulated Ca^{2+} Release. The rapidly decaying phase of cGMP-stimulated Ca^{2+} release is selectively inhibited by Na^+. The modulatory effect of Na^+ observed here is poised at free Na^+ levels of 5–10 mM. Somlyo and Walz (1985) demonstrated a light-induced reduction of the *total* Na^+ content of amphibian ROS, from 53 to 22 mM. On the basis of observations on other excitable cells [e.g., see Fozzard and Sheu (1980)], it is likely that much of the total Na^+ content of ROS is not free in cytoplasmic solution; if that is the case, then light-induced reduction of [Na^+] may potentiate the activity of this component of cGMP-stimulated cation flux. With the hypothesis that the biological role of the disk-associated channel is the rapid release of Ca^{2+} from disks, the suggestion would be that exposure of rods to light of sufficient intensity and duration to substantially lower cytoplasmic [Na^+] would *potentiate* this Ca^{2+} release activity. Thus, the Ca^{2+} release may be most active during the transition period from light to darkness, i.e, when cGMP levels rapidly reelevate but *before* ROS Na^+ levels recover.

A more detailed picture of the kinetics of reduction and reelevation of cGMP levels during photic stimulation of ROS would help determine when the putative disk-associated Ca^{2+} release activity would indeed be most active. To date, there have been qualitative demonstrations that cGMP levels transiently decline in ROS, but a quantitative picture of light-induced temporal and spatial changes in free cytoplasmic cGMP levels is difficult technically and has not yet been achieved. Furthermore, it has not yet been determined *whether and under what circumstances* a transient elevation of *cytoplasmic free* Ca^{2+} levels may occur. The tortuous cytoplasmic morphology defined by the dense lamellar packing of disks in ROS may promote spatial asymmetry in free cGMP and Ca^{2+} levels following changes in light intensity. Our data neither contradict nor compare with the prior observations in intact

rods of Schroder and Fain (1985); the latter were made on the time scale of minutes, vs the subsecond time scale reported here, and the latter measured net efflux of Ca^{2+} from the rod.

If the kinetics of cGMP-stimulated Ca^{2+} release observed here in vitro parallel the kinetics of a process that occurs in disks in vivo, the most likely consequence is a brief, transient period of Ca^{2+} release from the disks following reelevation of cGMP levels. Thus, the observations reported here raise the hypothesis that *cGMP-stimulated Ca^{2+} release activity in disks would be most active during the reelevation of cGMP levels following a light-stimulated decline*, due to the dual effect of reduction of cytoplasmic [Na^+] and reactivation of "inactivated" channels. This would be consistent with a possible role of Ca^{2+} in dark and/or light adaptation.

Added in Proof

Since this paper was submitted, a report appeared (Koch et al., 1987) which also demonstrates multiple functionally and pharmacologically distinct forms of cGMP-sensitive channels in ROS. These investigators employed purified, osmotically lysed ROS and measured Ca^{2+} release over a time course of several minutes using Ca^{2+}-sensitive fluorescent indicator. Since the time scale we employed was much faster, a direct comparison of the two sets of data cannot be made, but their results are at least qualitatively compatible with our own.

Acknowledgments

We thank Katherine L. Puckett for generously showing L.B.P. the method for preparation of disks and for helpful discussions. We also thank Kathleen J. Sweadner, Timothy J. Turner, and Robert L. Barnes for helpful comments on the manuscript.

Registry No. cGMP, 7665-99-8; Ca, 7440-70-2; Na, 7440-23-5.

References

Amis, E. J., Davenport, D. A., & Yu, H. (1981) *Anal. Biochem. 114*, 85–91.

Antonenko, Y. N., & Iaguzhinski, L. S. (1983) *Biofizika 28*, 1022–1025.

Baylor, D. A., Lamb, T. D., & Yau, K.-W. (1979) *J. Physiol. (London) 288*, 589–611.

Bensadoun, A., & Weinstein, D. (1976) *Anal. Biochem. 70*, 241–250.

Boyd, N. D. (1987) *J. Physiol. (London)* (in press).

Caretta, A., & Cavaggioni, A. (1983) *Eur. J. Biochem. 132*, 1–8.

Changeux, J. P., & Revah, F. (1987) *Trends Neurosci. (Pers. Ed.) 6*, 245–250.

Cook, N. J., Zeilinger, C., Koch, K.-W., & Kaupp, U. B. (1986) *J. Biol. Chem. 261*, 17033–17039.

Cook, N. J., Hanke, W., & Kaupp, U. B. (1987) *Proc. Natl. Acad. Sci. U.S.A. 84*, 585–589.

Draper, C., & Smith, K. (1966) *Applied Regression Analysis*, Wiley, New York.

Fain, G. L., & Lisman, J. E. (1981) *Prog. Biophys. Mol. Biol. 37*, 91–147.

Fain, G. L., & Schroder, W. H. (1985) *J. Physiol. (London) 368*, 641–665.

Fesenko, E. E., Kolesnikov, S. S., & Lyubarsky, A. L. (1985) *Nature (London) 313*, 310–313.

Forbush, B. (1984) *Anal. Biochem. 140*, 495–505.

Fozzard, H. A., & Sheu, S. S. (1980) *J. Physiol. (London) 273*, 579–586.

Furman, R. E., & Tanaka, J. C. (1987) *Biophys. J. 51*, 17a.

Goldin, S. M., & Sweadner, K. S. (1975) *Ann. N.Y. Acad. Sci. 264*, 387–397.

Goldin, S. M., Pearce, L. B., Burns, P. R., & Vincent, A. (1987) *Invest. Opthalmol. Visual. Sci. 28 (Suppl.)*, 95.

Haynes, L. W., Kay, A. R., & Yau, K. W. (1986) *Nature (London) 321*, 66–68.

Hess, P., Lansman, J. B., & Tsien, R. W. (1984) *Nature (London) 311*, 538–544.

Kaczorowski, G. J., Barros, F., Dethmars, J. K., & Trumble, M. J. (1985) *Biochemistry 24*, 1394–1403.

Kasahara, M., & Hinkle, P. C. (1977) *J. Biol. Chem. 252*, 7384–7390.

Kaupp, U. B., & Schnetkamp, P. P. M. (1982) *Cell Calcium 3*, 83–112.

Koch, K.-W., & Kaupp, U. B. (1985) *J. Biol. Chem. 260*, 6788–6800.

Koch, K.-W., Cook, N. J., & Kaupp, U. B. (1987) *J. Biol. Chem. 262*, 14415–14421.

Lamb, T. D. (1986) *Trends Neurosci. (Pers. Ed.) 9*, 224–227.

MacInnes, D. A. (1939) *The Principles of Electrochemistry*, Van Nostrand-Reinhold, New York.

Matesic, D., & Liebman, P. A. (1987) *Nature (London) 326*, 600–603.

McNaughton, P. A., Cervetto, L., & Nunn, B. J. (1986) *Nature (London) 322*, 261–263.

Miller, C., & Racker, E. (1979) in *The Receptors*, Vol. 1, pp 1–31, Plenum, New York.

Miller, D. L., & Korenbrot, J. I. (1986) *Neurosci. Res. (N.Y.), Suppl. 4*, S11–S34.

Miller, R. J. (1987) *Science (Washington, D.C.) 235*, 46–52.

Neubig, R. R., Boyd, N. D., & Cohen, J. B. (1982) *Biochemistry 21*, 3460–3467.

Nicol, G. D., Schnetkamp, P. P. M., Saimi, Y., Cragoe, E. J., Jr., & Bownds, M. D. (1987) *J. Gen. Physiol.* (submitted for publication).

Nilius, B., Hess, P., Lansman, J. B., & Tsien, R. W. (1985) *Nature (London), 316*, 443–446.

Nowycky, M. C., Fox, A. P., & Tsien, R. W. (1985) *Nature (London) 316*, 440–443.

Puckett, K. L., & Goldin, S. M. (1986) *Biochemistry 25*, 1739–1746.

Puckett, K. L., Aronson, E. T., & Goldin, S. M. (1985) *Biochemistry 24*, 390–400.

Schnetkamp, P. P. M. (1987) *Biochemistry 26*, 3249–3252.

Schroder, W. H., & Fain, G. L. (1984) *Nature (London) 309*, 268–270.

Siegl, P. K. S., Cragoe, E. J., Jr., Trumble, M. J., & Kaczorowski, G. J. (1984) *Proc. Natl. Acad. Sci. U.S.A. 81*, 3238–3242.

Somlyo, A. P., & Walz, B. (1985) *J. Physiol. (London) 358*, 183–195.

Stern, J. H., Kaupp, U. B., & MacLeish, P. R. (1986) *Proc. Natl. Acad. Sci. U.S.A. 83*, 1163–1167.

Stryer, L. (1986) *Annu. Rev. Neurosci. 9*, 87–119.

Wier, W. G., Cannell, M. B., Berlin, J. R., Marban, E., & Lederer, W. J. (1987) *Science (Washington, D.C.) 235*, 325–328.

Williams, D. A., Becker, P. L., & Fay, F. S. (1987) *Science (Washington, D.C.) 235*, 1644–1648.

Yau, K.-W., & Nakatani, K. (1985a) *Nature (London) 317*, 252–255.

Yau, K.-W., & Nakatani, K. (1985b) *Nature (London) 313*, 579–582.

Zimmerman, A. L., & Baylor, D. A. (1986) *Nature (London) 321*, 70–72.